Molecular Vision 2005; 11:169-78 <http://www.molvis.org/molvis/v11/a19>
Received 11 June 2004 | Accepted 16 February 2005 | Published 2 March 2005

Expression and immunolocalization of plasma membrane calcium ATPase isoforms in human corneal epithelium

Ernest F. Talarico, Jr.,[1] Brian G. Kennedy,[2] Carl F. Marfurt,[1] Karin U. Loeffler,[3] Nancy J. Mangini[1]

Departments of [1]Anatomy & Cell Biology and [2]Cellular & Integrative Physiology, Indiana University School of Medicine-Northwest, Gary, IN; [3]Department of Ophthalmology, University of Bonn, Bonn, Germany

Purpose: Plasma membrane Ca^{2+}-ATPases (PMCAs) are integral membrane proteins essential to the control of intracellular Ca^{2+} ($[Ca^{2+}]_i$) concentration. Four genes encode PMCA proteins termed PMCA1-PMCA4. Little is known about the expression of these isoforms in corneal epithelium (CE). The purpose of this investigation is to characterize the expression and distribution of PMCAs in human CE (hCE).
Methods: PMCA mRNA expression was examined by RT-PCR analysis of total RNA from native hCE using PMCA gene specific primers. PMCA isoform expression at the protein level in native hCE was examined by immunoblotting using isoform specific antibodies (Abs) and a panPMCA Ab that recognizes all PMCAs. Distribution of PMCAs in postmortem and surgical sections of hCE was determined by immunohistochemistry with the same Abs.
Results: Immunoblot analysis with the panPMCA Ab yielded an intense band of approximately 135 kDa and several faintly staining bands above and below this major band. The isoform specific Abs labeled one or more bands that corresponded to bands detected with the panPMCA Ab. RT-PCR analysis of total RNA from hCE yielded PCR DNAs that were identified by sequencing as products of PMCA1, PMCA2, PMCA3, and PMCA4, thus confirming the immunoblot data. Immunohistochemistry demonstrated localization of PMCAs in all layers of hCE. PMCA4 was the predominant isoform, and was expressed along the plasma membrane of cells in all layers of CE, except with a notable absence along the basal cell membranes adjacent to the stroma. PMCA1 and PMCA2 were found mainly on basal and wing cells. In contrast to PMCA4, PMCA1 immunoreactivity (IR) was located on portions of basal cell plasma membranes adjacent to the stroma. PMCA2 IR was detected cytoplasmically within basal and wing cells in both central cornea and limbus. PMCA3 IR was located in basal cell nuclei in central cornea, but in a perinuclear location in the limbal, basal, and wing cells.
Conclusions: Human CE expresses multiple PMCA isoforms that are differentially expressed and localized among the layers and cells that comprise the CE. We propose that the differential expression of multiple PMCA isoforms affords CE the requisite flexibility to respond to the demands for Ca^{2+} regulation required during renewal and regeneration of its multiple cell types.

Ca^{2+} plays multiple roles in biological systems acting both as an intracellular second messenger, and as a key factor (extracellularly) in adhesion and movement. Three calcium pumping ATPase systems operate to maintain cytosolic Ca^{2+} concentration ($[Ca^{2+}]_i$) at a low level of about 10^{-7} M [1-6]. These include ATPases localized in Golgi and related vesicular compartments, sarco/endoplasmic reticulum ATPases (SERCAs) that sequester Ca^{2+} into internal release compartments [7-11], and plasma membrane Ca^{2+}-ATPases (PMCAs) located in the surface membrane of cells that extrude Ca^{2+} against a large concentration gradient [12,13]. Thus, PMCAs also function to regulate extracellular $[Ca^{2+}]$ and play a critical role in Ca^{2+} homeostasis.

In humans, four genes (ATP2B1-ATP2B4) encode PMCA proteins termed PMCA1-PMCA4, respectively [14-18]. PMCA isoform diversity is increased via alternative splicing of primary RNA transcripts [16,19-23] that could result in more than 25 distinct proteins [7,20]. Although all PMCAs extrude cytosolic Ca^{2+} from cells, the different isoforms and splice variants are regulated differentially and have distinct biochemical properties [24]. Several studies show that PMCA isoform expression and location vary among cell types with respect to tissue specific calcium handling requirements [25-27]. Furthermore, PMCA dysregulation has been described in diseased cells and models of pathological conditions including sensorineural deafness, diabetes, and hypertension [28]. For example, PMCA2 is found in auditory and vestibular hair cells, where stimuli produce sudden calcium influxes during transduction that requires rapid extrusion to maintain responsiveness; an absence of PMCA2 in mice results in deafness and ataxia [26]. PMCA1 is expressed in all cells and tissues and its absence leads to embryonic lethality. By contrast, absence of PMCA4, which is also ubiquitously expressed, leads to male infertility [29]. Thus, we reasoned that determining which PMCA isoforms are expressed in CE and cataloging their location would help to understand the role of calcium pumps in maintaining corneal epithelial integrity and their possible involvement in corneal pathology.

The cornea comprises the anterior surface of the eye and is its principle refracting structure. The corneal epithelium (CE), a nonkeratinized, stratified squamous epithelium, is the outermost layer and forms a barrier against intraocular penetration of airborne pathogens and tear fluids [30-34]. CE also

Correspondence to: Nancy J. Mangini, Indiana University School of Medicine-Northwest, 3400 Broadway, Gary, IN, 46408-1197; Phone: (219) 980-6556; FAX: (219) 980-6566; email: nmangini@iun.edu

plays a role in stromal dehydration and the maintenance of corneal transparency, contributing approximately 3% of the total dehydration capacity [35]. Transepithelial Cl^- transport, coupled to water movement, can potentially thin a swollen stroma [36]. Critically, Cl^- transport mechanisms may be regulated by $[Ca^{2+}]_i$ [32,37].

In order to maintain its barrier function, the CE must be able to repair itself following wounding. The process of CE wound healing is complex, and involves a coordinated sequence of physiological events including cell migration, proliferation, and differentiation [38], all of which depend on calcium mediated processes. Concerning PMCA involvement, a wound healing study in the mouse [39] showed that during cell migration at the wound margin PMCAs redistributed from plasma membrane caveolae to membranous structures in the cytoplasm. PMCAs returned to the cell membrane when the defect was healed. Though $[Ca^{2+}]_i$ was not measured, this redistribution of PMCAs suggests that $[Ca^{2+}]_i$ may fluctuate during the wound healing process. In addition, changes in $[Ca^{2+}]_i$ could function in the regulatory program that directs changes in cell motility, morphology, and adhesion that are central to the wound healing process.

Reinach et al. [37,40,41] characterized Ca^{2+}-stimulated, Mg^{2+}-dependent ATPase activity and Ca transport in bovine CE. These early experiments are significant in that they demonstrated the presence of calmodulin sensitive Ca^{2+}-stimulated, Mg^{2+}-dependent ATPase activity in bovine corneal epithelial cells. Previously, there had been no reports in bovine CE of high affinity Ca^{2+}-stimulated ATPase activity, whose activity could maintain intracellular Ca^{2+} in the submicromolar range. The corneal epithelium is a complex system, and Reinach's work suggests the presence of more than one Ca^{2+}-stimulated, Mg^{2+}-dependent ATPase activity.

To completely define PMCAs and their roles in corneal biology, the molecular identity and physiological activity of these entities must be characterized. The goal of the present work was to lay the foundation for this analysis by examining, for the first time, expression, distribution, and cellular localization of different PMCA isoforms in CE. Clarifying the activity, location and splice variants of PMCA are critical to understanding the role(s) of PMCA in corneal epithelial cell biology.

We have examined both human eye bank corneas and eyes obtained immediately after enucleation and keratoplasty. We report that all four PMCA isoforms are expressed in hCE, and that the isoforms are distributed differentially in the CE cell layers. We propose that the differential expression of PMCA isoforms in CE reflects fundamental differences in calcium regulation requirements in this continuously regenerating epithelium.

METHODS

Experiments were conducted according to the guidelines of the Institutional Review Board of Indiana University School of Medicine and in compliance with federal regulations governing the use and protection of human subjects in research.

Sources of human donor eyes: Corneas from human cadavers and living donors used in this investigation were from three sources: National Disease Research Interchange (Philadelphia, PA), Central Florida Lions Eye Bank (Tampa, FL), and the Department of Ophthalmology, University of Bonn (Bonn, Germany). The age of donor, presence of any ocular pathology, and time to fixation are reported in appropriate sections below.

Antibodies: Monoclonal antibodies (Abs) 5F10 and JA9, and polyclonal Abs NR1, NR2, and NR3 were generously donated by Affinity BioReagents, Inc. (Golden, CO) and have been previously characterized [23,42,43]. 5F10 is a "panPMCA" Ab that recognizes a highly conserved epitope near the PMCA active site that is found in all four PMCA isoforms. Ab JA9 is specific for PMCA 4 [23,42,43]. NR1, NR2, and NR3 are epitope affinity purified, rabbit polyclonal IgG Abs that detect specifically PMCA1, PMCA2, and PMCA3, respectively [23,43]. Secondary Abs were from Vector Laboratories (Burlingame, CA).

Sample preparation for immunoblotting: CE cells for immunoblotting studies were obtained from eleven donors. One combined sample (03-041c) was comprised of CE scraped from four donor corneas ranging in age from 57-76 years. The second combined sample (03-048c) was comprised of CE collected from seven donors ranging in age from 63-76 years. In all cases, donors had no known history of ocular pathology.

CE was removed by mechanical scraping while immersed in ice cold 0.1 M PBS (0.084 M Na_2HPO_4, 0.016 M KH_2PO_4, 0.9% NaCl). The cells were placed into a conical centrifuge tube, suspended by gentle pipetting, and centrifuged at 180x g for 7 min. The cell pellet was resuspended and washed in 1X PBS (130 mM NaCl, 2.5 mM KCl, 8 mM Na_2HPO_4, 1.5 mM KH_2PO_4), centrifuged as before, and resuspended in 50 µl of 0.1 M PBS. An aliquot was removed for determination of total protein concentration by the Lowry Assay [44]. The remaining suspension was solubilized in 500 µl of electrophoresis sample buffer consisting of 2% SDS, 10% glycerol, 200 mM HEPES (pH 6.8), 1 mM EDTA, 0.1% bromophenol blue, 5% mercaptoethanol, 20 µl Protease Inhibitor Cocktail (Sigma, St. Louis, MO) and 20 µl Complete Protease Inhibitor (Roche, Indianapolis, IN), and stored at -20 °C. CE samples and molecular weight standards were resolved by SDS-PAGE using a Laemmli system with an 8% gel [45-47] as described previously for retinal pigment epithelium [48]. Proteins were transferred to PVDF membranes (Immobilon-P, Millipore, Burlington, MA) by semi-dry electroblotting. Protein transfer to the blot was assessed by staining with Ponceau S (Sigma).

Immunoblotting: Blots were wet with MeOH, washed using a high salt Tris Buffered Saline Solution (HTBS; 500 mM NaCl; 25 mM Tris base, pH 7.5), and blocked for 2 h at RT, with SuperBlock® Blocking Buffer (Pierce TBS Dry Blend; Pierce, Rockford, IL). After a wash in HTBS containing 0.2% Tween 20 (HTBS-Tw), blots were reacted with primary Ab for 2 h at RT, with gentle agitation. Primary Abs were diluted 1:10,000 (5F10), or 1:2,500 (JA9, NR1, NR2, and NR3) in HTBS containing 0.4% blotting grade nonfat dry

milk (Bio-Rad Laboratories, Hercules, CA) and 0.2% Tween 20. The blots were then washed four times in HTBS-Tw, blocked a second time in Pierce SuperBlock® for 2 h at RT, and incubated for 2 h at RT with secondary Ab (horse anti-mouse or goat anti-rabbit IgG) conjugated to alkaline phosphatase (Vector Laboratories). Secondary Abs were diluted in the same vehicle used for primary Abs. The blots were then washed four times in HTBS-Tw, and incubated for 30 min at RT in CDP-Star chemiluminescent substrate (Applied Biosciences, Bedford, MA) in order to visualize the cross-reacting bands. The chemiluminescent signal was captured using a Kodak Image Station 440CF (Kodak, Rochester, NY) and 1D Image Analysis Software.

Control blots for NR1, NR2, or NR3 were incubated with antibodies preabsorbed with an excess of the respective immunizing peptide using the manufacturer's suggested protocol (Acris Antibodies, Hiddenhausen, Germany). Briefly, antibody-peptide mixtures were prepared with a 28 fold excess of peptide to antibody and incubated for 2 h at 37 °C, then for 24 h at 4 °C. The mixture was centrifuged at 15,000 rpm at 4 °C for 15 min. The supernatant was partially decanted, leaving 5-10 µl in the tube, which was then diluted 1:2500 for immunoblotting studies or 1:1000 for immunohistochemistry experiments.

RNA preparation and RT-PCR: CE from five donors ranging in age from 55-76 years was collected by mechanical scraping as previously described and placed into RNALater™ (Ambion, Austin, TX). Total RNA for each donor was extracted using RNAqueous-4PCR (Ambion) including DNase treatment of the final RNA pellet. Total RNA was reversed transcribed using oligo-dT primers and SuperScript™ First Strand Synthesis for RT-PCR Kit (Invitrogen, Carlsbad, CA). Negative controls included omission of reverse transcriptase. PCR amplification was performed using a GeneAmp PCR System 2700 (Applied Biosciences), 1 µl of first-strand DNA, 400 nmol of PMCA gene primers, and the High Fidelity PCR Master Kit (Roche) in a final reaction volume of 25 µl. Presence of transcripts for PMCA1 (NM_001682), PMCA2 (NM_001683.2), PMCA3 (NM_001001344), and PMCA4 (NM_001684) was tested using the PMCA primers listed in Table 1. Cycling conditions were as follows; initial denaturation at 94 °C for 2 min, then 35 cycles of 94 °C for 10 s, 55 °C for 30 s and 72 °C for 1 min, with a final extension at 72 °C for 7 min. PCR DNAs were analyzed using a Rapid Agarose Gel Electrophoresis System (RGX60, Biokey American Instrument, Inc., Portland, OR) in 2.0% agarose gels in 1X TAE buffer (8 min at 210 V). PCR DNAS were either gel purified or subcloned and then sequenced by the CRC DNA Sequencing Facility, University of Chicago.

Table 1. PMCA primers used for RT-PCR

Gene	Name	Sequence (5'-3')
PMCA1	HPMCA1P-sense	TTCAACGAAATAAATGCCCGG
	HPMCA1M-antisense	AGGGTGGAGGACTGGAGTTACG
PMCA2	P2PbeWo-sense	ACAGTGGTACAGGCCTATGTCG
	P2cam-antisense	CGAGTTCTGCTTGAGCGCGG
PMCA3	P3cap-sense	TGTCCACAGAACAGTGGCTC
	P3cam-antisense	ATGCCGCTGTCTATGGCGTT
PMCA4	P4cap-sense	CAACTCCCGAAAGATCCATG
	P4cam-antisense	TGGTTAACACAGCAGCTGAC

PMCA primers were designed to be isoform specific and to flank the putative B and C splice sites [21].

Immunohistochemistry of postmortem specimens: Corneal tissue from four donor corneas, two female and two male, ranging in age from 23-66 years, were frozen and sectioned for fluorescence immunohistochemistry. Of these, one cornea was remarkable for mild arcus, while the other three demonstrated no specified ocular pathology. Approximate time from enucleation to fixation was 17 to 20 h. On delivery, donor corneas used for immunohistochemistry were placed in ice cold 0.1 M PBS and trimmed of excess tissue except for a thin rim (about 1.0 mm) of sclera. The center of each cornea was marked, and then the cornea was cut into quadrants using a number 10 scalpel blade. The quadrants were immersion fixed for 30 min at RT in 4% paraformaldehyde containing 0.2% picric acid and 2% sucrose in 0.1 M PBS, pH 7.3, and then passed through a series of graded sucrose solutions (5%, 10%, 20%, and 30% sucrose in 0.1 M PBS) for at least 1 h each at 4 °C. Tissues were stored in ice cold 30% sucrose-PBS until sectioned. Prior to sectioning, quadrants were placed epithelial side up on a microscope slide, a small piece of tissue was cut from one edge of the quadrant extending from limbus to central cornea and placed into OCT Compound (Tissue-Tek®; Sakura Finetechnical Co., Torrance, CA) for 20 min and then frozen. Sections perpendicular to the corneal surface were cut at eight microns on a Minitome cryostat (Triangle Biomedical, Durham, NC) and collected onto chrome-alum-gelatin coated slides.

Sections were washed three times in 0.1 M PBS at RT, incubated for 20 min in ice cold MeOH and washed three times in 0.1 M PBS-0.3% Triton X-100 (TX100). Sections were incubated for 20 min at RT in the appropriate blocking serum (10% normal horse or goat serum [NHS or NGS], Vector Laboratories) in 0.1 M PBS-0.3% TX100, then incubated overnight at 4 °C in primary Ab solution containing 10% normal serum in 0.1 M PBS-0.3% TX100. 5F10 was applied at a final dilution of 1:5,000, while PMCA isoform specific antibodies (JA9, NR1, NR2, and NR3) were used at dilutions of 1:1,000. Sections were washed three times in 0.1 M PBS-0.3% TX100 and then incubated with Fluorescein (FITC) conjugated secondary Ab (horse anti-mouse IgG or goat anti-rabbit IgG, diluted 1:100) for 60 min at RT in a humidified chamber. After a final wash, the slides were coverslipped with SlowFade Mounting Medium (Molecular Probes, Eugene, OR). Negative controls included incubation of adjacent sections with primary Abs preabsorbed with immunizing peptides as described in the section above on immunoblotting and incubation of sections in nonimmune mouse IgG.

Immunohistochemistry of surgical specimens: PMCA localization was also examined in paraffin sections of two human surgical corneal specimens. One cornea was obtained from an eye that had been enucleated secondary to choroidal melanoma from a 54-year-old male, and the second cornea was

removed from the eye of a 66-year-old female who had undergone keratoplasty for Fuchs' Endothelial Dystrophy. Corneal specimens were embedded in paraffin, sectioned at 20 μm on a rotary microtome and collected onto slides. The sections were incubated for 2.5 days at 4 °C in primary Ab diluted in TBS, pH 7.6, containing 1% BSA (dilutions: NR1, 1:800; NR2, 1:1,600; NR3, 1:300, and JA9, 1:400). Immunoreactivity was visualized using biotinylated rabbit or mouse secondary Abs and streptavidin-biotin horseradish peroxidase complexes (StreptABComplex/HRP Duet, Mouse/Rabbit; Dako, Glostrup, Denmark) with aminoethylcarbazol as the chromogen. Controls included omission of primary antisera and incubation with nonimmune rabbit or mouse sera.

Digital imaging microscopy: The presence and distribution of each PMCA isoform was evaluated with reference to two epithelial regions: (1) corneal limbus and (2) central cor-

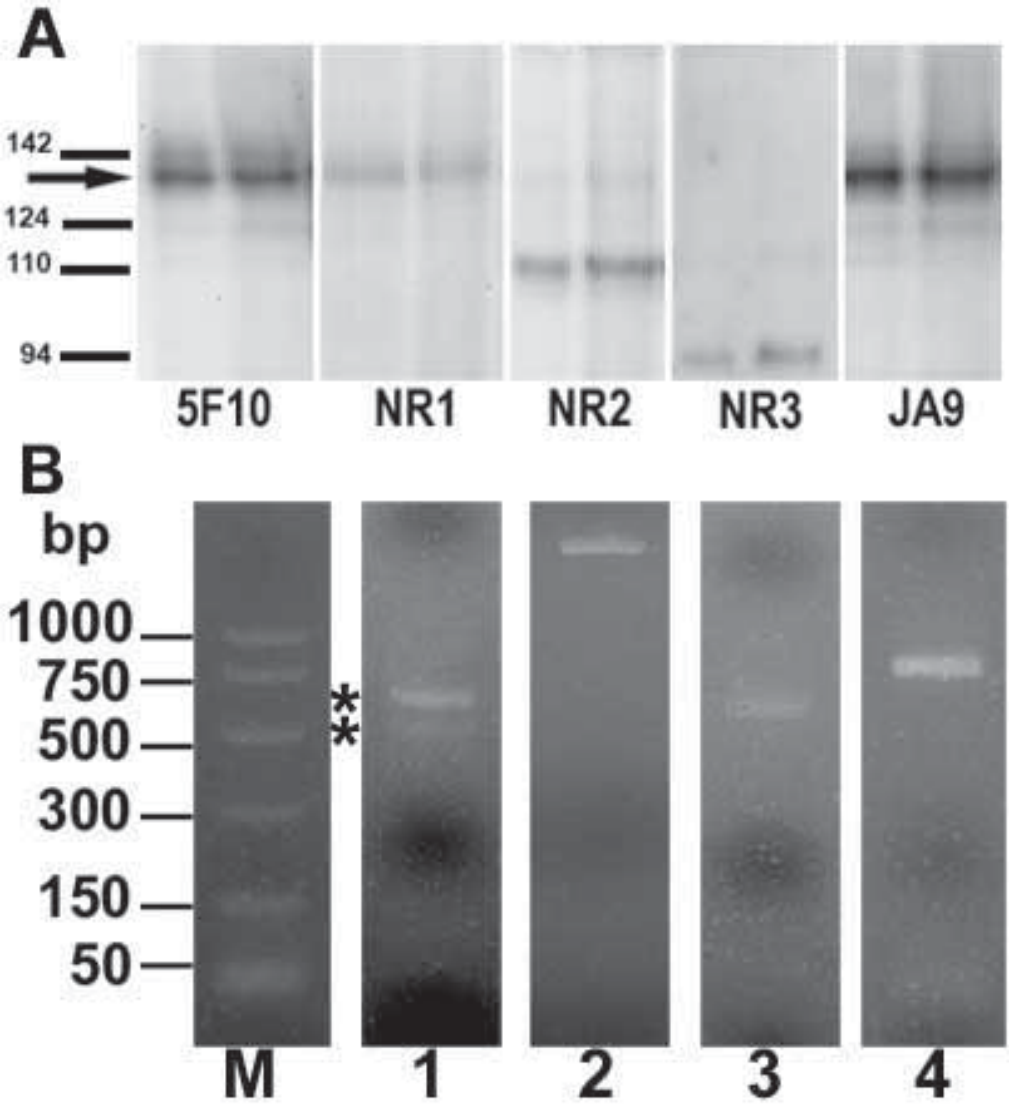

Figure 1. Isoform expression in native human corneal epithelium (hCE). **A**: Immunoblot analysis of PMCA isoforms in hCE. Blot lanes were loaded with equal aliquots (about 20 μg protein) from two different samples of whole cell lysates of hCE. The panPMCA antibody (5F10) intensely labeled a band at about 135 kDa (arrow) and additional bands above and below that size (identified by markers to the left of the lane). Isoform specific PMCA antibodies (NR1, NR2, NR3, and JA9) detected bands that comigrated with one or more of the bands labeled by 5F10. 5F10 was used at 0.65 mg/ml. All other antibodies were used at 0.4 mg/ml. **B**: RT-PCR analysis of PMCA isoforms in human hCE. Total RNA extracted from native hCE was used for RT-PCR with specific primers across sites B and C for PMCA1, PMCA2, PMCA3, and PMCA4 (lanes 1, 2, 3, and 4, respectively). All lanes represent products obtained from second round PCR reactions. Lane M is PCR size markers. PCR products were separated by agarose gel electrophoresis and stained with ethidium bromide. PCR products were either gel purified or subcloned, then sequenced. In all cases, sequencing identified these products as the respective PMCA isoforms. Specifically, PCR amplification of PMCA1 (lane 1) yielded two fragments of 593 and 487 bp, respectively (asterisks). Sequences were identical to published sequences for human splice variants PMCA1b and PMCA1kb. PCR amplification of PMCA2 yielded fragments of 1,640 bp (lane 2, 99% identical to human PMCA2a) and 1,147 bp (not shown, a putative PMCA2kb splice variant). PCR amplifications of PMCA3 and PMCA4 each yielded a single fragment (lane 3; 632 bp and lane 4; 805 bp, that corresponded to PMCA3a and PMCA4b, respectively).

nea. The borders of the limbus seen in section perpendicular to the surface are approximated by drawing a line between the terminations of Bowman's layer and Descemet's membrane, and a second line parallel and 1 mm peripheral to the first line. The central cornea is the area extending from the limbus to the corneal apex. Images were captured by epifluorescent or brightfield microscopy using a Magnifier CCD camera (Olympus, Melville, NY) and processed using Adobe Photoshop.

RESULTS

Immunoblot analyses of PMCAs in whole cell lysates of native hCE: Data from an immunoblotting experiment examining two different, pooled samples of hCE are shown in Figure 1A. The results with all antibodies were identical between the two samples. Specifically, the panPMCA Ab (5F10) intensely labeled a band at approximately 135 kDa (Figure 1A, arrow) and additional faint bands that migrated above and below the main band. In the case of isoform specific antibodies, blots incubated with anti-PMCA1 (NR1) or anti-PMCA4 (JA9) detected bands that comigrated with the major band labeled by 5F10. JA9 also detected fainter bands at approximately 124 kDa and 110 kDa, similar to bands seen on the 5F10 blot. Anti-PMCA2 (NR2) strongly labeled a band at approximately 110 kDa and a minor band at approximately 135 kDa. Anti-PMCA3 (NR3) labeled a band at about 94 to 100 kDa. The relative signal intensity of IR with JA9 suggested that the major isoform expressed in both samples of hCE was PMCA4. In blots incubated with primary Abs preabsorbed with the respective isoform specific immunizing peptides (i.e., preabsorption control), the labeled band(s) were diminished in intensity or not detected (data not shown).

Immunoblot data suggested that hCE expressed all four PMCA isoforms. These data were validated by mRNA analysis using PMCA isoform gene specific primers that demonstrated the presence of PCR DNAs in hCE encoding all four PMCA isoforms (Figure 1B).

Localization of PMCAs in postmortem corneal specimens: Fluorescent immunohistochemistry employing a panPMCA Ab and isoform specific Abs was used to assess PMCA localization in hCE. IR was observed with all Abs but the pattern of distribution varied.

PanPMCA labeling: Cryostat sections of corneas from four postmortem eyes were examined using the panPMCA Ab, 5F10. The data presented in Figure 2 are from the cornea of a 63-year-old, male donor (time from enucleation to fixation, 14.5 h) and are representative of the results. Specifically, 5F10 strongly labeled the plasma membranes of cells in all layers and in all regions of the CE (Figure 2A). The corneal stroma was unstained. Every frozen section of human cornea examined in this study demonstrated an identical pattern of 5F10 labeling. Control sections incubated with nonimmune mouse IgG were unstained (Figure 2B).

Isoform specific labeling: Immunoblotting and molecular data showed that all four isoforms were expressed (Figure 1A,B). To determine how these isoforms contributed to the pattern of 5F10 IR (Figure 2A), tissues sections were reacted with isoform specific PMCA Abs (Figure 3) .

Incubation with PMCA1-, PMCA2-, and PMCA3 specific Abs (NR1, NR2, and NR3, respectively), produced modest staining mainly in the basal epithelial cell layer and more diffuse staining in wing cell and squamous cell layers in the central cornea (Figure 3A-E). Figure 3B-F show sections incubated with isoform specific PMCA Abs preabsorbed with

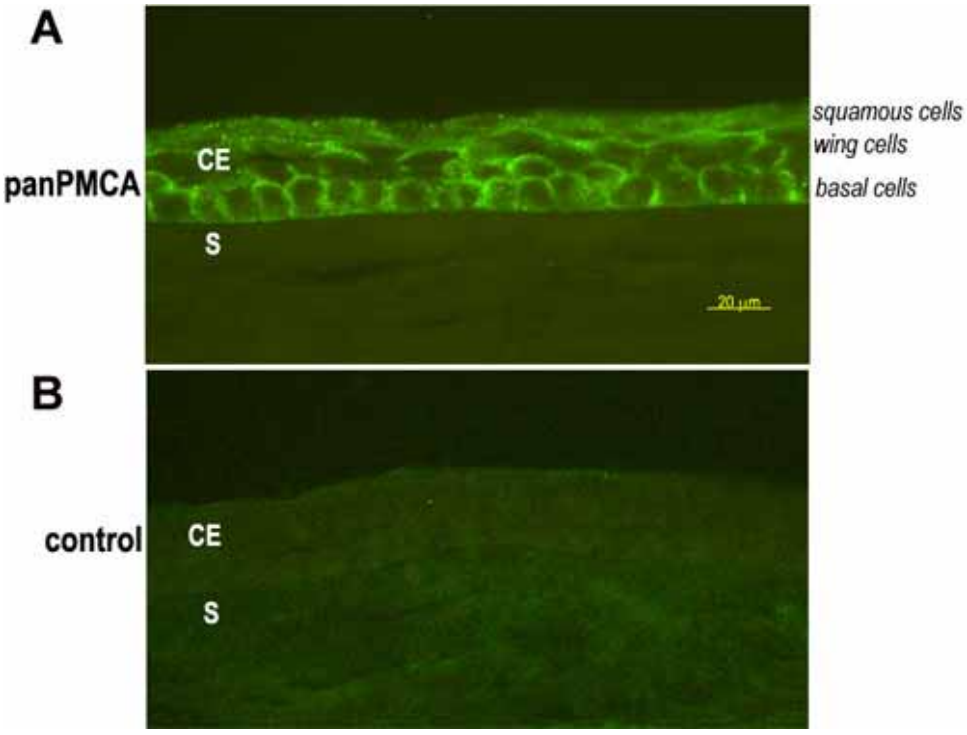

Figure 2. Localization of PMCA in human corneal epithelium. **A**: Immunostaining with pan-PMCA antibody (5F10) revealed strong PMCA labeling in all layers of the corneal epithelium (CE). The staining was associated primarily with the plasma membranes. The stroma (S) was unstained. **B**: Control section incubated with nonimmune mouse IgG was unstained.

the respective immunizing peptides (i.e., preabsorption controls). In a preabsorption control, IR may be reduced but not completely eliminated, as was the case in this experiment. Sections incubated with nonimmune mouse IgG (negative controls) were unstained (Figure 3H).

Tissue sections incubated with PMCA4 Ab (JA9) showed intense fluorescence principally along the plasma membranes of cells in all layers of CE (Figure 3G). The pattern of PMCA4 IR was similar to that observed with the panPMCA Ab (Figure 2A) with one notable exception. That is, labeling with 5F10 was detected all around basal cells, while labeling with JA9 was largely absent along the basal cell membrane of a large percentage of basal cells (arrows, Figure 3G).

Localization of PMCAs in surgical corneal specimens: When using postmortem tissue, it is difficult to control the interval between the time of death and processing of tissue. Thus, paraffin embedded sections of corneas from surgical specimens were examined using isoform specific antibodies and streptavidin-biotin immunohistochemistry. Findings from surgical specimens were similar to those described above for postmortem specimens (Figure 4).

In sections of surgical specimens, PMCA1 in hCE was localized primarily to the plasma membranes of basal cells, and to a lesser extent, wing cells in the central cornea (Figure 4A). In the limbus, PMCA1 was located mainly in the cytoplasm of suprabasal cells (Figure 4B). The relative intensity

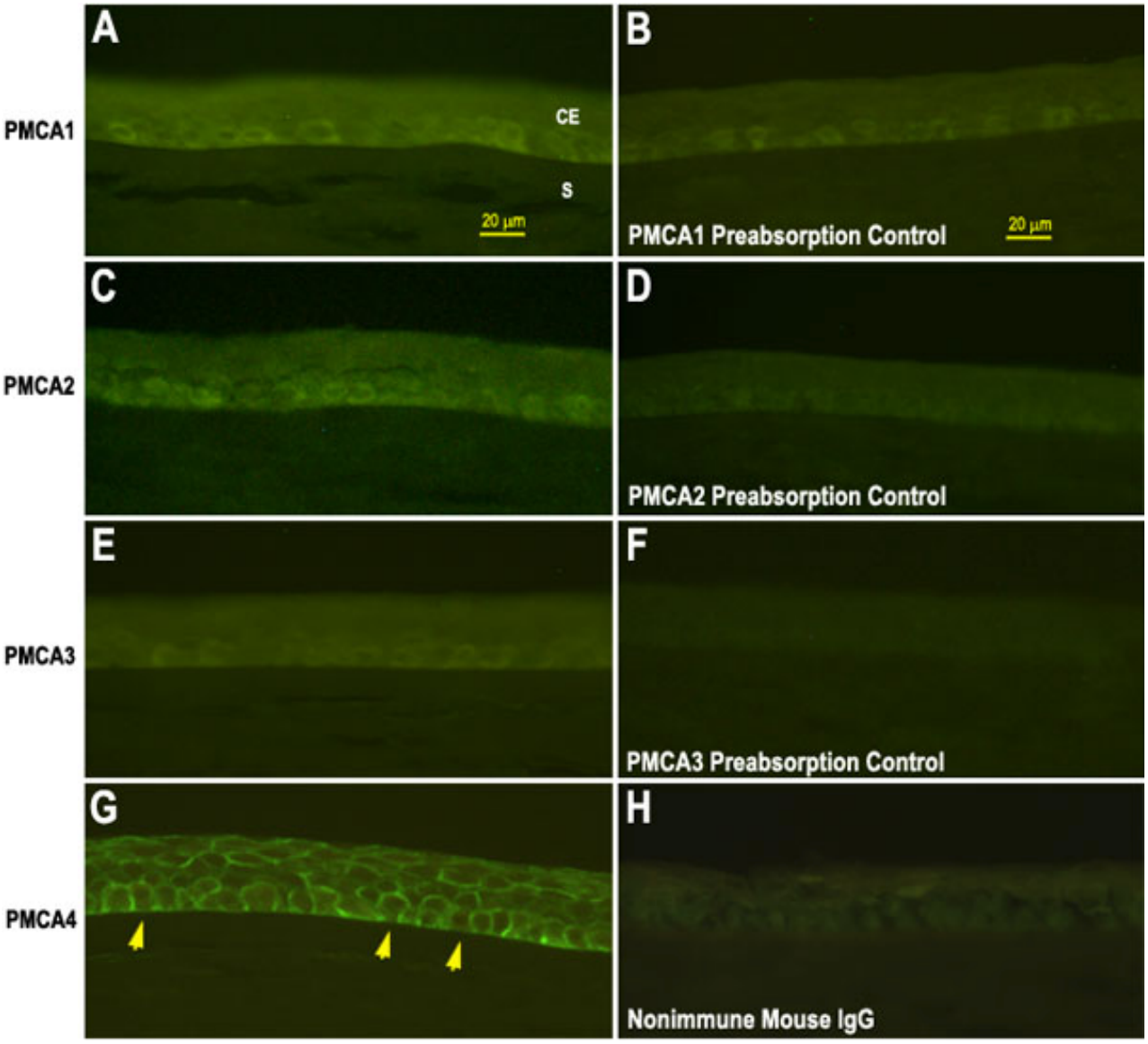

Figure 3. Localization of PMCA isoforms in frozen sections of human corneal epithelium from postmortem specimens. Immunostaining with isoform specific PMCA antibodies showed that PMCA1 (**A**), PMCA2 (**C**), and PMCA3 (**E**) were found primarily in basal cells. PMCA4 IR was localized to plasma membranes in the squamous, wing and basal cell layers, but was lacking along the basal cell membrane adjacent to the stroma (**G**, arrows). Controls included preabsorption of primary antibodies with the appropriate immunizing peptide for PMCA1 (**B**), PMCA2 (**D**), PMCA3 (**F**), or incubation with nonimmune IgG for JA9 (**H**). Staining was reduced or eliminated in all control conditions. The bars in (**A**) and (**B**) represent 20 µm and apply to all panels. The corneal epithelium (CE) and the stroma (S) are labeled in panel **A**.

of IR in the limbus was greater than that observed in the central cornea. The squamous cell layer in both the central cornea and limbus appeared to lack PMCA1 IR.

Immunostaining for PMCA2 showed diffuse cytoplasmic labeling of basal cells and wing cells in both the central cornea (Figure 4C) and limbus (Figure 4D). There appeared to be no difference in relative intensity of IR for PMCA2 between these two regions.

PMCA3 IR in surgical sections was detected in basal cell nuclei in the central cornea (Figure 4E) and in the perinuclear regions of basal and wing cells of the limbus (Figure 4F). The presence of PMCA3 IR was not detected in squamous cells of either the central cornea or the limbus.

Immunoreactivity for PMCA4 was clearly detected on the plasma membrane of cells in all layers of the central cornea (Figure 4G) and limbus (not shown). Intense labeling was

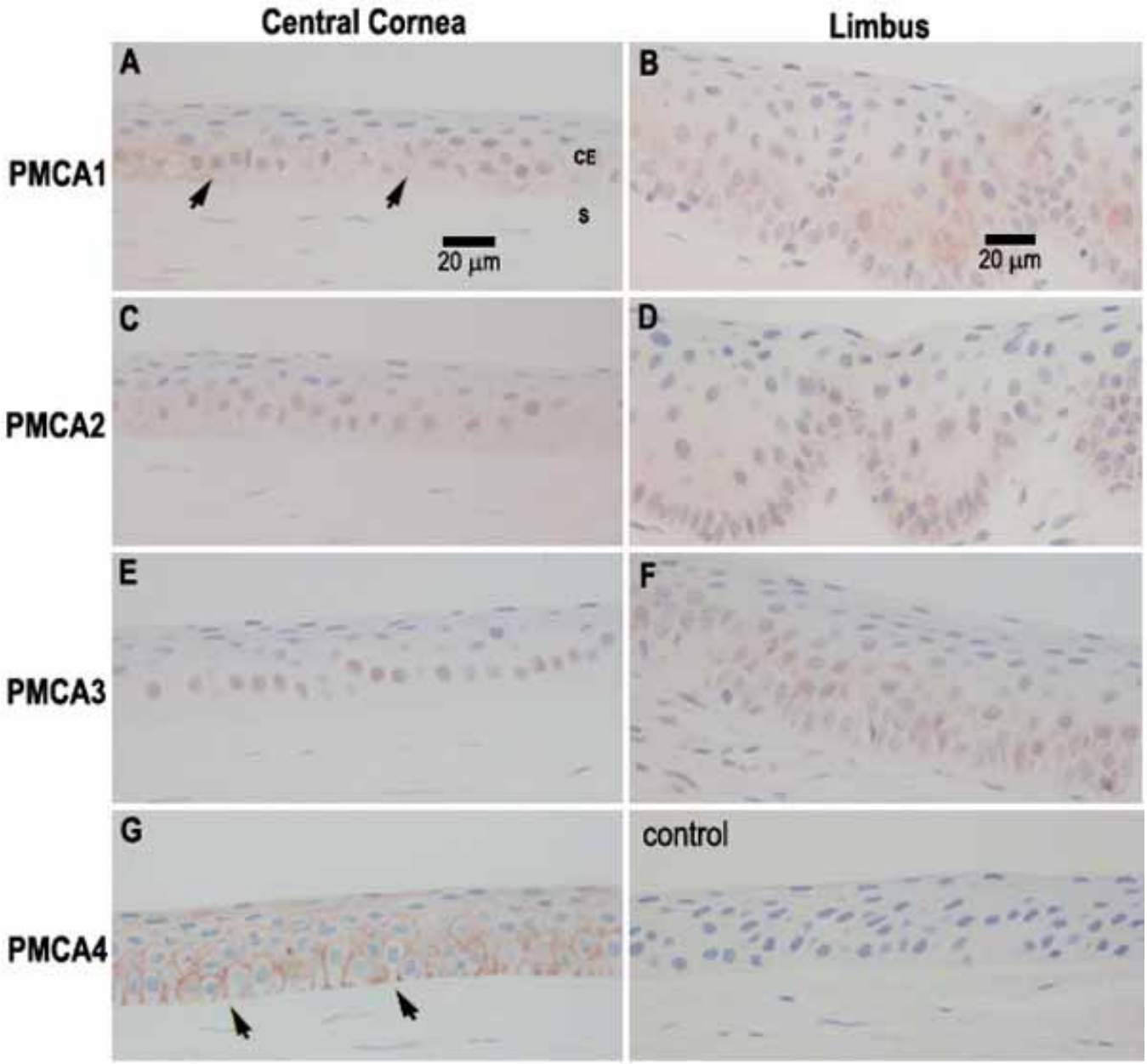

Figure 4. Localization of PMCA Isoforms in paraffin sections of human corneal epithelium from surgical specimens. PMCA1 was found mainly on basal cells in central cornea including the plasma membrane facing the stroma (**A**; arrows), and in the cytoplasmic domain of basal, and especially wing cells, in the limbus (**B**). PMCA2 was located mainly on cytoplasmic membranes in basal and wing cells of both central cornea (**C**) and limbus (**D**). PMCA3 IR was observed on basal cell nuclei in central cornea (**E**) and in perinuclear regions of basal and wing cells in the corneoscleral limbus (**F**). PMCA4 IR was prominent on plasma membranes of cells in all layers of corneal epithelium (**G**), but appeared to be lacking from most basal cell plasma membranes facing the stroma (**G**; arrows). Sections reacted with nonimmune rabbit or mouse sera were unstained (the mouse control is shown). Bars in **A** and **B** represent 20 μm and apply to all panels. The corneal epithelium (CE) and the stroma (S) are labeled in panel **A**.

observed along the lateral basal cell plasma membranes, but little IR was apparent along the basal aspect of basal cell plasma membranes facing the stroma (arrows, Figure 4G). IR was absent in control sections that were incubated with omission of primary antisera or incubation with nonimmune rabbit or mouse sera. Overall, PMCA4 IR was the greatest of all the isoforms examined, again suggesting that PMCA4 was the major isoform present in hCE.

DISCUSSION

The results of this study show, for the first time, the presence and distribution of plasma membrane calcium ATPases in human corneal epithelium. Immunoblot studies, mRNA analysis and immunocytochemistry of postmortem and surgical corneal specimens demonstrated the presence of all four PMCA isoforms. CE is a complex tissue comprised of cells that are undergoing continual renewal, migration, and differentiation. We suggest that the CE requires multiple PMCA isoforms, each with unique regulatory properties, in order to accommodate the different Ca^{2+} mediated signaling processes that underlie these different events.

Immunoblotting data (Figure 1A) showed that all four PMCA isoforms are expressed in human corneal epithelium. The intense IR of the major band on blots incubated with anti-PMCA4 Ab further suggested that PMCA4 is the major isoform expressed in CE. Our immunoblot findings were validated by molecular experiments demonstrating the presence of PCR DNAs encoding all four PMCA isoforms (Figure 1B) in native hCE. PMCA4 product was always observed following first round PCR; other products were detected subsequent to second round PCR. This suggested that similar to protein studies, PMCA4 mRNA was the predominate isoform expressed in hCE.

Immunolocalization data demonstrated that the PMCA isoforms exhibited a differential distribution among corneal epithelial cell layers and, in some instances, a different pattern of staining between central cornea and limbus. Specifically, the panPMCA Ab intensely labeled the plasma membranes of all cells in all layers. Of the isoform specific antibodies, PMCA4 labeling most closely resembled the pattern and intensity of panPMCA labeling, again suggesting that PMCA4 is the major isoform expressed within human CE.

Immunohistochemical studies further demonstrated that in basal epithelial cells, PMCA4 IR was expressed on lateral and apical cell membranes, but not on the basal cell membranes abutting the corneal stroma (Figure 3G and Figure 4G). The functional significance of this polarized distribution remains to be determined. However, we suggest that PMCA4 could play a role in stabilizing cell to cell junctions. For example, E-cadherin is found in cell membranes of corneal epithelial cells [49]. In the classical cadherin model, extracellular Ca^{2+} first interacts within pockets located in E-cadherins resulting in the formation of rigid E-cadherin dimers. Under the influence of additional Ca^{2+}, these dimers bind adjacent cells together by forming E-cadherin oligomers [50]. PMCA4 could function to stabilize these adhesions by pumping Ca^{2+} into the junctional space. This idea is supported by one study showing that PMCAs redistribute from cell membrane caveolae to cytoplasmic membranes during reepithelialization of CE following wounding [39]. This excision of PMCAs from the cell membrane would decrease free Ca^{2+} in the junctional space available to interact with E-cadherins, resulting in more flexible cell to cell adhesions, and thus allowing for ease of cell migration during corneal wound healing.

PMCA1 was observed primarily in corneal basal epithelial cells. Surgical specimens showed that in contrast to PMCA4, some PMCA1 was localized to basal cell membranes adjacent to the stroma. Building on the model suggested for PMCA4, we propose that PMCA1 in this location may play a role in the development and/or maintenance of cell to extracellular matrix adhesion mechanisms. Studies show that Ca^{2+} transients play a role in adhesion formation and release during cell migration [51]. Basal cells in the CE are not static; they migrate centripedally and then move superficially as they differentiate. To do this, there must exist a plastic relationship between adhesion and the ability of basal cells to move that is likely to be Ca^{2+} dependent.

In addition to their interaction with the underlying stroma, basal cells of the CE are unique in that they maintain their proliferative activity. The CE is a continuum of cells that arise from the basal cells and end in terminally differentiated squamous cells, and is renewed and replaced entirely every 12-14 days [52-54]. Stem cells located in the limbus differentiate into basal cells during their migratory journey from the limbus into the cornea proper. This may be significant in that the intensity of PMCA1 IR appeared to be greater in limbal epithelium (Figure 4B) as compared to the epithelium of the central cornea (Figure 4A), suggesting differences in the calcium handling needs of the cells that comprise limbal epithelium.

PMCA2, like PMCA1, is expressed mainly in basal cells, with lesser amounts in the wing cell layers in the central cornea and limbus. As with PMCA1, little to no label was present in squamous cell layers, suggesting a lesser role for PMCA2 in terminally differentiated cells of the CE.

Minimal PMCA3 labeling was detected in CE. Specifically, PMCA3 IR was located mainly in basal cells of the central cornea in both postmortem and surgical tissue sections. Interestingly, PMCA3 IR in frozen sections from postmortem specimens was located in extranuclear areas of basal cells, whereas in paraffin embedded, surgical specimens label was seen only on the nuclei of basal cells in central cornea. Additionally, in the limbus of surgical specimens, PMCA3 IR was evident in perinuclear regions of basal and wing cells. This is the only instance in this study where there was an apparent difference in the pattern of PMCA IR between postmortem and surgical corneal specimens. It is not clear whether methodological differences or postmortem changes contributed to this result. Of interest, nuclear labeling with PMCA3 Ab (NR3) was also observed in cultured human corneal epithelial cells (unpublished observation).

This is the first report of PMCA localization in human corneal epithelium. The expression and differential distribution of multiple PMCA isoforms in CE suggests that Ca^{2+}-handling requirements differ among the cell types comprising

this stratified epithelium, and would allow the various cell types in the CE to maintain different baseline levels of $[Ca^{2+}]_i$, and to selectively respond to signals regulating $[Ca^{2+}]_i$. To fully understand calcium handling by the corneal epithelium, the transporters catalyzing calcium efflux must be characterized. To begin this process, the present work has examined PMCA expression in human corneal epithelium. Additional studies to understand the role of each PMCA isoform in corneal epithelial calcium handling are needed.

ACKNOWLEDGEMENTS

This research was supported by funds from Indiana University School of Medicine-Northwest, NIH Grant NEI ROI EY11308 (to NJM), and the Sigma XI Research Society (to EFT). The authors acknowledge the significant contributions of David M. Lubeck, MD, Arbor Center for EyeCare, Homewood, IL, and Affinity BioReagents, Inc., Golden, CO. Peptides for NR1, NR2, and NR3 were a generous gift from John T. Penniston and Adelaida Filoteo, Mayo Clinic, Rochester, MN. Parts of this work were presented at the 2004 Annual Meeting of the Association for Research in Vision and Ophthalmology, Ft. Lauderdale, FL and the 2004 Annual Meeting of the American Association of Anatomists, Washington, DC.

REFERENCES

1. Lytton J, Westlin M, Burk SE, Shull GE, MacLennan DH. Functional comparisons between isoforms of the sarcoplasmic or endoplasmic reticulum family of calcium pumps. J Biol Chem 1992; 267:14483-9.
2. MacLennan DH, Toyofuku T, Lytton J. Structure-function relationships in sarcoplasmic or endoplasmic reticulum type Ca2+ pumps. Ann N Y Acad Sci 1992; 671:1-10.
3. Shull GE, Clarke DM, Gunteski-Hamblin AM. cDNA cloning of possible mammalian homologs of the yeast secretory pathway Ca(2+)-transporting ATPase. Ann N Y Acad Sci 1992; 671:70-80; discussion 81.
4. Carafoli E, Longoni S. The plasma membrane in the control of the signaling function of calcium. Soc Gen Physiol Ser 1987; 42:21-9.
5. Carafoli E. Intracellular calcium homeostasis. Annu Rev Biochem 1987; 56:395-433.
6. Carafoli E, Stauffer T. The plasma membrane calcium pump: functional domains, regulation of the activity, and tissue specificity of isoform expression. J Neurobiol 1994; 25:312-24.
7. Brandt PC, Vanaman TC. The plasma membrane calcium pump: not just another pretty ion translocase. Glycobiology 1996; 6:665-8.
8. Guerini D, Carafoli E. The Calcium Pumps. In: Carafoli, E, Klee, C, editors. Calcium as a Cellular Regulator, New York: Oxford University Press; 1999. p. 229-278.
9. Gunteski-Hamblin AM, Clarke DM, Shull GE. Molecular cloning and tissue distribution of alternatively spliced mRNAs encoding possible mammalian homologues of the yeast secretory pathway calcium pump. Biochemistry 1992; 31:7600-8.
10. Antebi A, Fink GR. The yeast Ca(2+)-ATPase homologue, PMR1, is required for normal Golgi function and localizes in a novel Golgi-like distribution. Mol Biol Cell 1992; 3:633-54.
11. Virk SS, Kirk CJ, Shears SB. Ca2+ transport and Ca2+-dependent ATP hydrolysis by Golgi vesicles from lactating rat mammary glands. Biochem J 1985; 226:741-8.
12. DUNHAM ET, GLYNN IM. Adenosinetriphosphatase activity and the active movements of alkali metal ions. J Physiol 1961; 156:274-93.
13. Schatzmann HJ. ATP-dependent Ca++-extrusion from human red cells. Experientia 1966; 22:364-5.
14. Shull GE, Greeb J. Molecular cloning of two isoforms of the plasma membrane Ca2+-transporting ATPase from rat brain. Structural and functional domains exhibit similarity to Na+,K+- and other cation transport ATPases. J Biol Chem 1988; 263:8646-57.
15. Verma AK, Filoteo AG, Stanford DR, Wieben ED, Penniston JT, Strehler EE, Fischer R, Heim R, Vogel G, Mathews S Strehler-Page M-A, James P, Vorherr T, Krebs J, Carafol E. Complete primary structure of a human plasma membrane Ca2+ pump. J Biol Chem 1988; 263:14152-9.
16. Greeb J, Shull GE. Molecular cloning of a third isoform of the calmodulin-sensitive plasma membrane Ca2+-transporting ATPase that is expressed predominantly in brain and skeletal muscle. J Biol Chem 1989; 264:18569-76.
17. Brandt P, Zurini M, Neve RL, Rhoads RE, Vanaman TC. A C-terminal, calmodulin-like regulatory domain from the plasma membrane Ca2+-pumping ATPase. Proc Natl Acad Sci U S A 1988; 85:2914-8.
18. Brandt P, Vanaman TC. Splicing of the muscle-specific plasma membrane Ca(2+)-ATPase isoforms PMCA1c is associated with cell fusion in C2 myocytes. J Neurochem 1994; 62:799-802.
19. Strehler EE. Recent advances in the molecular characterization of plasma membrane Ca2+ pumps. J Membr Biol 1991; 120:1-15.
20. Kamagate A, Herchuelz A, Bollen A, Van Eylen F. Expression of multiple plasma membrane Ca(2+)-ATPases in rat pancreatic islet cells. Cell Calcium 2000; 27:231-46.
21. Stauffer TP, Hilfiker H, Carafoli E, Strehler EE. Quantitative analysis of alternative splicing options of human plasma membrane calcium pump genes. J Biol Chem 1993; 268:25993-6003. Erratum in: J Biol Chem. 1994; 269(50):32022.
22. Strehler EE, Strehler-Page MA, Vogel G, Carafoli E. mRNAs for plasma membrane calcium pump isoforms differing in their regulatory domain are generated by alternative splicing that involves two internal donor sites in a single exon. Proc Natl Acad Sci U S A 1989; 86:6908-12.
23. Filoteo AG, Elwess NL, Enyedi A, Caride A, Aung HH, Penniston JT. Plasma membrane Ca2+ pump in rat brain. Patterns of alternative splices seen by isoform-specific antibodies. J Biol Chem 1997; 272:23741-7.
24. Strehler EE, Treiman M. Calcium pumps of plasma membrane and cell interior. Curr Mol Med 2004; 4:323-35.
25. Borke JL, Caride AJ, Yaksh TL, Penniston JT, Kumar R. Cerebrospinal fluid calcium homeostasis: evidence for a plasma membrane Ca2+-pump in mammalian choroid plexus. Brain Res 1989; 489:355-60.
26. Dumont RA, Lins U, Filoteo AG, Penniston JT, Kachar B, Gillespie PG. Plasma membrane Ca2+-ATPase isoform 2a is the PMCA of hair bundles. J Neurosci 2001; 21:5066-78.
27. Krizaj D, Demarco SJ, Johnson J, Strehler EE, Copenhagen DR. Cell-specific expression of plasma membrane calcium ATPase isoforms in retinal neurons. J Comp Neurol 2002; 451:1-21.
28. Lehotsky J, Kaplan P, Murin R, Raeymaekers L. The role of plasma membrane Ca2+ pumps (PMCAs) in pathologies of mammalian cells. Front Biosci 2002; 7:d53-84.
29. Okunade GW, Miller ML, Pyne GJ, Sutliff RL, O'Connor KT, Neumann JC, Andringa A, Miller DA, Prasad V, Doetschman T,

Paul RJ, Shull GE. Targeted ablation of plasma membrane Ca2+-ATPase (PMCA) 1 and 4 indicates a major housekeeping function for PMCA1 and a critical role in hyperactivated sperm motility and male fertility for PMCA4. J Biol Chem 2004; 279:33742-50.
30. Cogan DG, Kinsey VE. The cornea: physiological aspects. Arch Ophthalmol 1942; 28:661-669.
31. Klyce SD. Electrical profiles in the corneal epithelium. J Physiol 1972; 226:407-29.
32. Klyce SD. Transport of Na, Cl, and water by the rabbit corneal epithelium at resting potential. Am J Physiol 1975; 228:1446-52.
33. Klyce SD, Crosson CE. Transport processes across the rabbit corneal epithelium: a review. Curr Eye Res 1985; 4:323-31.
34. Kenyon KR, Chaves HV. Morphology and pathologic response of corneal and conjunctival disease. In: Smolin G, Tofts RA, editors. The Cornea: Scientific Foundations and Clincal Practice. 3rd ed. Boston: Little, Brown; 1994. p. 69-114.
35. Joyce NC. Cell Biology of the Corneal Endothelium. In: Albert DM, Jakobiec FA, editors. Principles and practice of ophthalmology. Philadelphia: WB Saunders; 1994. p. 17-37.
36. Klyce SD. Enhancing fluid secretion by the corneal epithelium. Invest Ophthalmol Vis Sci 1977; 16:968-73.
37. Reinach PS. Roles of cyclic AMP and Ca in epithelial ion transport across corneal epithelium: a review. Curr Eye Res 1985; 4:385-91.
38. Thoft RA, Friend J. Permeability of regenerated corneal epithelium. Exp Eye Res 1975; 21:409-16.
39. Amino K, Honda Y, Ide C, Fujimoto T. Distribution of plasmalemmal Ca(2+)-pump and caveolin in the corneal epithelium during the wound healing process. Curr Eye Res 1997; 16:1088-95.
40. Reinach P, Holmberg N. Ca-stimulated Mg dependent ATPase activity in a plasma membrane enriched fraction of bovine corneal epithelium. Curr Eye Res 1987; 6:399-405.
41. Reinach PS, Holmberg N, Chiesa R. Identification of calmodulin-sensitive Ca(2+)-transporting ATPase in the plasma membrane of bovine corneal epithelial cell. Biochim Biophys Acta 1991; 1068:1-8.
42. Adamo HP, Caride AJ, Penniston JT. Use of expression mutants and monoclonal antibodies to map the erythrocyte Ca2+ pump. J Biol Chem 1992; 267:14244-9.
43. Caride AJ, Filoteo AG, Enyedi A, Verma AK, Penniston JT. Detection of isoform 4 of the plasma membrane calcium pump in human tissues by using isoform-specific monoclonal antibodies. Biochem J 1996; 316:353-9.
44. LOWRY OH, ROSEBROUGH NJ, FARR AL, RANDALL RJ. Protein measurement with the Folin phenol reagent. J Biol Chem 1951; 193:265-75.
45. Laemmli UK, Paulson JR, Hitchins V. Maturation of the head of bacteriophage T4. V. A possible DNA packaging mechanism: in vitro cleavage of the head proteins and the structure of the core of the polyhead. J Supramol Struct 1974; 2:276-301.
46. Laemmli UK, Quittner SF. Maturation of the head of bacteriophage T4. IV. The proteins of the core of the tubular polyheads and in vitro cleavage of the head proteins. Virology 1974; 62:483-99.
47. Laemmli UK, Teaff N, D'Ambrosia J. Maturation of the head of bacteriophage T4. III. DNA packaging into preformed heads. J Mol Biol 1974; 88:749-65.
48. Kennedy BG, Mangini NJ. Plasma membrane calcium-ATPase in cultured human retinal pigment epithelium. Exp Eye Res 1996; 63:547-56.
49. Takahashi M, Fujimoto T, Honda Y, Ogawa K. Distributional change of fodrin in the wound healing process of the corneal epithelium. Invest Ophthalmol Vis Sci 1992; 33:280-5.
50. Tepass U, Truong K, Godt D, Ikura M, Peifer M. Cadherins in embryonic and neural morphogenesis. Nat Rev Mol Cell Biol 2000; 1:91-100.
51. Cox EA, Huttenlocher A. Regulation of integrin-mediated adhesion during cell migration. Microsc Res Tech 1998; 43:412-9.
52. HANNA C, BICKNELL DS, O'BRIEN JE. Cell turnover in the adult human eye. Arch Ophthalmol 1961; 65:695-8.
53. HANNA C, O'BRIEN JE. Cell production and migration in the epithelial layer of the cornea. Arch Ophthalmol 1960; 64:536-9.
54. Cenedella RJ, Fleschner CR. Kinetics of corneal epithelium turnover in vivo. Studies of lovastatin. Invest Ophthalmol Vis Sci 1990; 31:1957-62.

The print version of this article was created on 2 Mar 2005. This reflects all typographical corrections and errata to the article through that date. Details of any changes may be found in the online version of the article.